JMEPEG (2004) 13:557–563
DOI: 10.1361/10599490419955

1059-9495/$19.00

Low Friction Stainless Steel Coatings Graphite Doped Elaborated by Air Plasma Sprayed

A. Harir, H. Ageorges, A. Grimaud, P. Fauchais, and F. Platon

(Submitted February 10, 2004)

A new process has been developed to incorporate graphite particles into a stainless steel coating during its formation. Four means have been tested to inject the graphite particles outside the plasma jet and its plume: graphite suspension, a graphite rod rubbed on the rotating sample, powder injection close to the substrate with an injector, or a specially designed guide. The last process has been shown to be the most versatile and the most easily controllable. It allows the incorporation of between 2 and 12 vol.% of graphite particles (2-15 μm) within the plasma sprayed stainless steel coatings. A volume fraction of 2% seems to give the best results with a slight decrease (6%) of the coating hardness. This volume fraction also gave the best results in dry friction on the pin-on-disk apparatus. Depending on the sliding velocity (0.1-0.5 m/s) and loads (3.7-28 N), the dry friction coefficient against a 100C6 pin is reduced by between 1.5 and 4 compared with that obtained with plasma sprayed stainless steel.

Keywords coefficient of friction, composite coatings, hardness, plasma spraying, stainless steel/graphite, wear resistance

1. Introduction

The incorporation of solid lubricants into coatings during the thermal spraying step can be used to produce self-lubricating surfaces having improved friction characteristics for applications involving sliding wear. Examples of studies are available in the literature in which coatings containing solid lubricants were produced by thermal spraying.[1-7] The main problem for these materials is the degradation of the solid lubricant during the spray process, for example, the reaction of the carbon with the oxygen of the entrained air. However, as a result of the short residence time of the particles in the plasma, and the special design of the composite particles containing the lubricant, it appears that a portion of the solid lubricant is deposited and becomes part of the coating. This has been observed in the case of sprayed powder blends containing Teflon or ethylene tetrafluoroethylene (ETFE) based material.[3,4] To protect the Teflon particles, which degrade at temperatures above 300 °C, from the high temperatures, a ceramic cladding of alumina-titania serves as a thermal barrier. This limits the degradation of the polymer particles. Using this approach, abradable coatings (Ni-C, AlSi-Polymer, AlSi-C) with low hardness (i.e., between 25 and 82 $HV_{0.1}$) have been obtained with good coefficient of friction values when tested against a steel substrate (34CrMo3 with a hardness of 200 $HV_{1.5}$) under certain loads and relative velocities.[6] When spraying FeCSi with different volume fractions of CaF_2, good friction results were obtained up to 800 °C, pro-vided the powders were sprayed by supersonic air-gas plasmas.

To summarize, good results can be obtained when spraying particles containing solid lubricants, such as C, CaF_2, polytetrafluoroethylene (PTFE) or ETFE, if steps are taken to limit the heat transfer of the plasma to the particles so as to limit the decomposition of the solid lubricant portion of the particle. Besides, if there is too much of the nonmelting phase within the coatings, its cohesion becomes poor and the friction bad as soon as the load increases. The goal of this work is to develop a process whereby a solid lubricant can be introduced in the coating between successive passes without heating and, thus, decomposing it. After a short description of the experimental setup, the tribological results obtained using four different graphite (2-15 μm in diameter) introduction processes to produce a stainless steel coating sprayed onto an alumina alloy are presented and discussed.

2. Experimental Procedures

2.1 Plasma Spray Apparatus

Plasma sprayed coatings were realized with an experimental setup described in detail elsewhere,[7] using a PTF4-type torch (nozzle internal diameter: 7 mm). Spraying was performed in air with a gas mixture of argon/hydrogen: 45/15 slm and an arc current of 530 A, resulting in a voltage of 62 V (32 kW with a thermal efficiency of 56%).

The disk-shaped substrates (40 mm in diameter, 8 mm in thickness) were made of aluminum alloy and grit blasted to a R_a roughness equal to 7 ± 1 μm. Six disks were arrayed on a rotating substrate holder 110 mm in diameter. The standoff distance was 100 mm. The substrate holder was continuously rotated at 2.5 rev/s, while being simultaneously translated back

A. Harir, H. Ageorges, A. Grimaud, and **P. Fauchais,** Laboratoire de Sciences des Procédés Ceramiques et de Traitements de Surface (SPCTS) UMR-CNRS 6638 Université de Limoges 123 av. A. Thomas 87060 Limoges Cedex, France; and **F. Platon,** Groupe d'Études des Matériaux Hétérogénes (GEMH) – ENSCI 47 av. A. Thomas 87065 Limoges, France. Contact e-mail: helene.ageorges@unilim.fr; fauchais@unilim.fr.

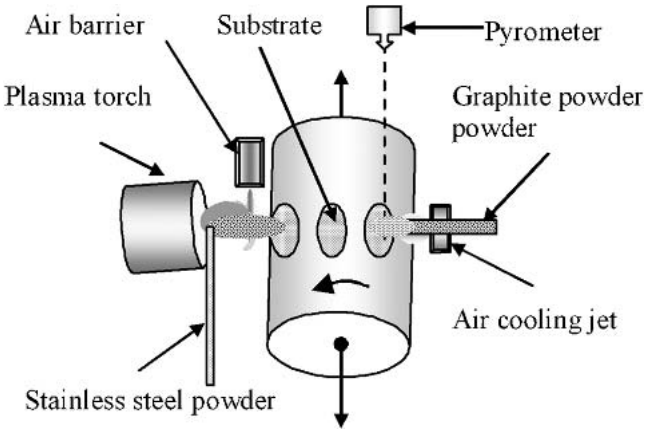

Fig. 1 Scheme of the experimental setup

and forth, orthogonally to the plasma jet axis, at a velocity of 20 mm/s. The excursion distance was 80 mm (the plasma torch being stationary). The substrate temperature, and hence that of the deposit, could be held constant during spraying with an air barrier blown orthogonally to the jet axis at a distance of 20 mm from the substrate.

The 316L stainless steel particles (60-130 μm) were injected into the gas stream, using a vibrating powder feeder with 3 slm of argon as the carrier gas, perpendicular to the axis of the plasma jet, 3 mm downstream of the torch nozzle exit through an injector 2 mm in diameter. The stainless steel powder flow rate was fixed to 80 g/min. The substrate and coating temperature was kept at 150 °C according to previous tests.[9] The coating thickness was 500 μm.

Four different means were used to inject the graphite particles within the stainless steel coating during its formation:

- A suspension of graphite particles (2-15 μm) in acetone was used with the suspension droplets being created by a spray painting gun positioned opposite of the plasma torch and directed at the substrate holder.
- A rod of graphite was continuously rubbed over the coating surface opposite of the plasma torch.
- Graphite particles with a size distribution in the range 2-15 μm were injected as shown in Fig. 1. The powder feeder consisted of a fluidized bed where particles were elutriated and continuously vibrated. The exit hole of the alumina injection tube (internal diameter of 4 mm) was located at a point 30 mm from the substrate surface.
- The same device as described in (3) was used, but the injection tube was extended to the coating surface by a device specially designed to guide graphite particles up to a few tenths of mm from the surface.

2.2 The Tribometer

The tribometer used for tribology tests was a pin-on-disk type. The pin was made of 100C6 steel. It consisted of a shouldered cylinder with the friction surface having a diameter of 6 mm. The disk was the composite deposit, millstone corundum rectified (R_a equal to ~1.7 μm), and rotated at a constant speed (Fig. 2). Two conditions of sliding speed were used (0.1 and 0.5 m/s) with three different applied normal static loads (N equal to 12, 18, and 28 N). The pin was connected to a cell so that the applied torque could be monitored. The friction coefficient was calculated using the relationship:

$$f = \frac{C}{N\,R}$$

where R is the mean radius of the friction track (16 mm in this case), N is the applied load, and C is the applied torque.

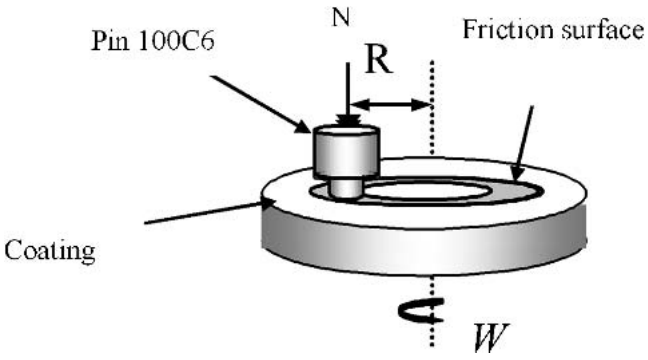

Fig. 2 Tribological test configuration: pin on disk

Table 1 Properties of Plasma Sprayed Stainless Steel (316L) Coatings

SS316L	Structure	Oxide	Hardness	Porosity
Properties	Lamellar	CrO ≈ 2 wt.%	190 ± 30	9%

Table 2 Dry Friction Coefficient of Stainless Steel 316L Against 100C6 Steel

Sliding Velocity, m/s	Normal Load, N	Mean Friction Coefficient	
		Sprayed SS	Bulk SS
0.1	11.7	0.55	0.59
	18	0.61	0.5
	28	0.6	0.98
0.5	11.7	0.46	…
	18	0.68	…
	28	0.59	…

2.3 Other Characterizations and Analysis Devices

The quality of the coatings was determined by scanning electron microscopy (SEM). Energy dispersive spectroscopy (EDS) was used to detect the presence of graphite. The percentage of graphite in the deposit was determined either by image analysis or with a C/H/N analyzer.

The microhardness measurements of the coatings were performed on polished cross sections using a Vickers hardness (HV) tester with a load of 5 N applied for 15 s. Twenty measurements of microhardness were averaged to determine their mean value. The porosity was measured by the Archimedian method.

3. Results and Discussion

3.1 Stainless Steel Coatings

The properties of stainless steel (55) coatings are summarized in Table 1. The high oxide content is probably due to the convection movment induced within the particles during their flight in the plasma jet core (first 40 to 50 mm).[10] The coating friction properties are given in Table 2, together with those obtained with bulk stainless steel. In general, the friction coefficient f is higher for bulk SS than for sprayed SS. This can be explained by examining the friction track, which for sprayed SS is covered by a third body made of stainless steel resulting from the degradation of the lamellar structure. This third body is not observed to the same extent on track on bulk SS.

Table 3 Mean Values of the Wear Coefficient (10^{-12} Pa^{-1}) of Coatings for a 0.1 m/s Sliding Velocity

Load, N	SS Coating Wear	Composite Coating Wear
11.7	3.86	4.08
18	0.6	5.59

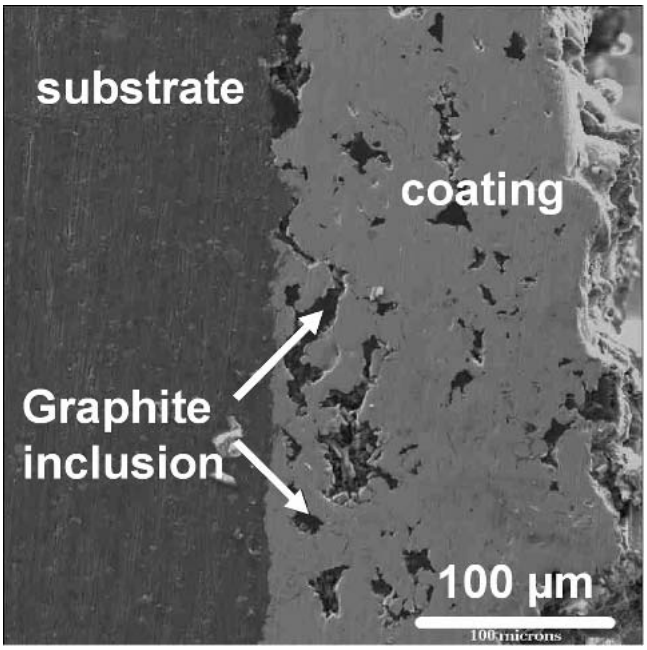

Fig. 3 Polished cross section of a SS-graphite coating obtained by rubbing a graphite rod on the coating surface during its formation

3.2 Composite Coatings Through a Graphite Suspension

The spray-painting gun is designed for precision operations; i.e., it allows low mass flow rates (a few g/min) of the suspension and disperses it in rather narrow strips (~20 mm). Two suspensions have been used containing 27 and 15 wt.% of graphite, and these were sprayed at a distance of between 50 and 150 mm from the substrate. In all cases, the resulting coatings were almost pure stainless steel with a small quantity of carbon. The porosity was between 10% and 20%. Thus, the coating hardness is lower than those of pure SS (between 140 and 170 HV_2 compared with 186 HV_2). In all cases, the friction coefficient of the composite coating is higher (between 10% and 20%) than that of the pure SS. When observing the friction track, wear debris was observed. The wear debris results from the much higher deterioration of the composite coating than that of the pure SS. This is due to the preheating temperature of the substrate during spraying which is higher than the vaporization temperature of acetone, and it results in the incorporation within the coating of liquid suspension droplets, which are completely vaporized. This leads to the high porosity.

3.3 Composite Coatings Through Graphite Rod Abrasion

The next development of the process was to rub continuously on the coating, opposite to the spray torch, a graphite rod.

Table 4 Mean Values of the Friction Coefficient for Different Test Conditions

Normal Load and Rotational Speed Applied	Friction Coefficient	
	Steel	Steel + Graphite
11.7 N, 0.1 m/s	0.59	0.40
18 N, 0.1 m/s	0.61	0.40
28 N, 0.1 m/s	0.60	0.45
11.7 N, 0.5 m/s	0.46	0.36
18 N, 0.5 m/s	0.68	0.45
28 N, 0.5 m/s	0.59	0.36

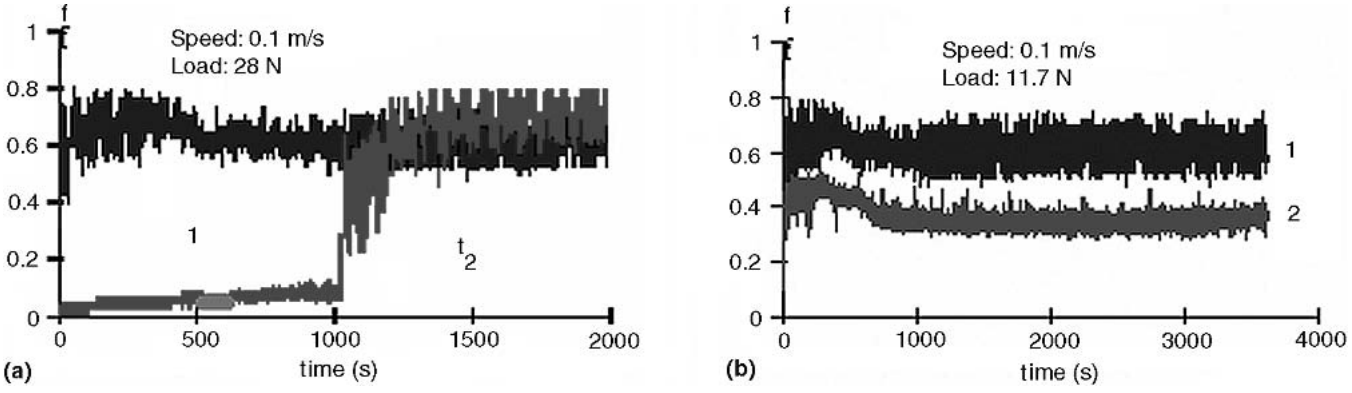

Fig. 4 Time evolution of the friction coefficients of stainless steel (1) and composite coatings (2) for two different loads **(a)** 28 N and **(b)** 11.7 N

Graphite inclusions are uniformly distributed within the SS coating as shown in Fig. 3. However, the hardness is very low (about 80 ± 18 compared with 190 ± 30 for the SS). Depending on the friction conditions (Table 2), the friction coefficient is reduced by 10-30%. Unfortunately, as soon as the load is increased the wear of the coating becomes drastic as shown in Table 3.

3.4 Composite Coatings Through Graphite Injection

The most difficult step has been the design of a powder feeder adapted to graphite particles (2-15 μm), i.e., a vibrated fluidized bed where the particles are elutriated. The distance between the alumina injection tube and the coating is also a key parameter. If it is too close, the graphite is blown off of the substrate. If it is too far, the graphite becomes too dispersed. A good compromise seems to be a distance of 20 mm. However, it is very difficult to control the quantity of graphite incorporated within the coating with 80-90 wt.% of the injected graphite being blown off by the graphite carrier gas. Coatings achieved in these conditions contain graphite inclusions randomly distributed but with a volume fraction less than 1%, which is far from the 10 wt.% injected. The coating hardness is 173 ± 23, which is close to that of pure SS. The evolution of the friction coefficient f of the composite deposits of stainless steel-graphite, compared with those of a pure stainless steel, is seen in Fig. 4. For all tribology test conditions (three loads for two different speeds), the friction coefficient of the composite coatings is lower than that of pure steel coatings. According to the load conditions and test duration, this reduction is in the order of 30-50% (Table 4).

The analysis of the material collected from the friction track for the test conditions indicated in Fig. 4(a) for the region of

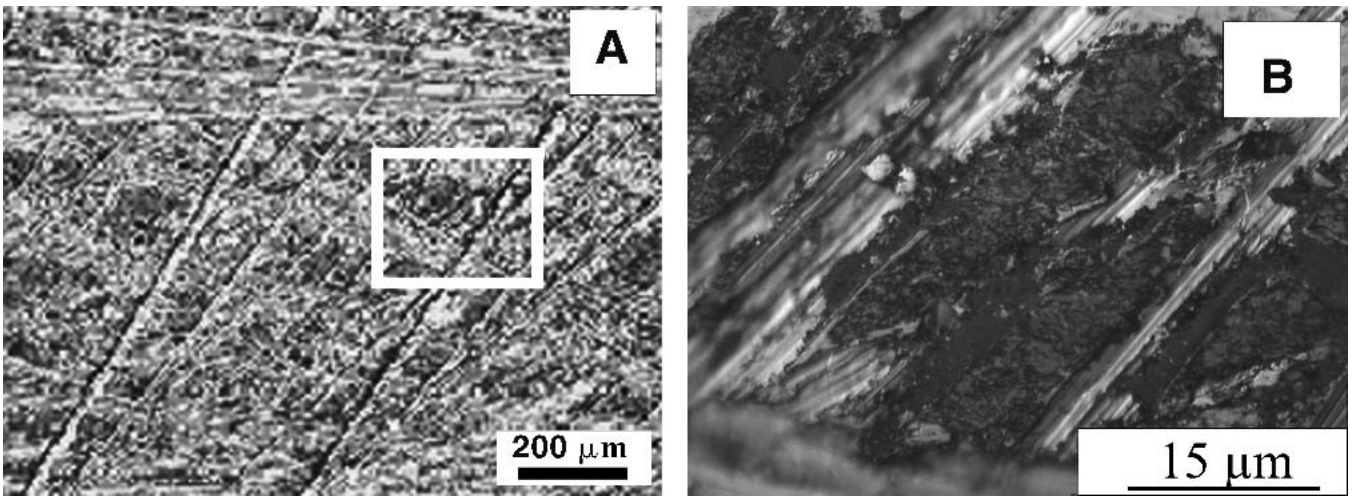

Fig. 5 SEM picture **(a)** of the friction track during the low friction step shown in Fig. 4(a) and **(b)** the rubbed pin

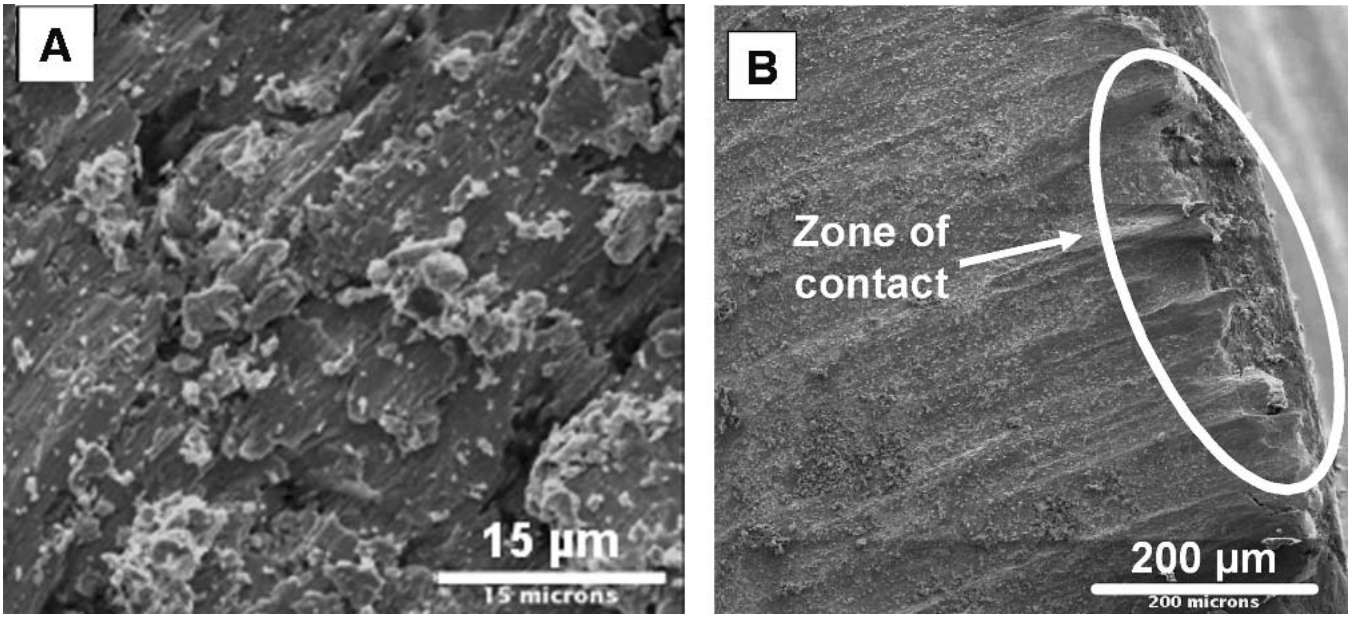

Fig. 6 SEM pictures of **(a)** track of friction, **(b)** rubbed pin

low friction at the beginning of the test shows that the third body consists of compacted graphite lamellae in contact with the lift zones (Fig. 5). In this case, the reduction in the friction coefficient is due to the formation of graphite lamellae that permit the adaptation of the speeds at the level of the third body by shearing of the graphite lamellae.[11,12]

During this phase, the graphite lubricates the contacts.[13,14] Its action is time limited and also related to the volumetric fraction of graphite within the metallic matrix. The formation of graphite lamellae is only possible when the topography of the surfaces in contact exhibits very weak roughness and good planarity, which is not really the case in these experiments. During the test, the elimination of the graphite films can occur if the quantity of graphite in the composite is low, resulting in interactions between the metal of the pin and the metal of the matrix. The pull-out of the graphite particles deteriorates the contact surfaces and limits the formation of graphite transfer films (Fig. 6a). This situation results in a fast transition of the friction coefficient, shifting it from low to high values (Fig. 4a). In this second stage of wear, the third body is a mixture of metallic and graphite particles.

If the geometry of the contact at the beginning of the test promotes metallic material adhesion, the low friction phase no longer appears (Fig. 4b). Nevertheless, the value of the friction coefficient of the composite deposit is still lower by 50% relative to that obtained with the steel deposit. The graphite particles present in the third body particles modify the tribological behavior of the contact. The geometric shortcomings of the pin and the disk promote localized contacts (Fig. 6b), resulting in local contact pressures much higher than the theoretical one.

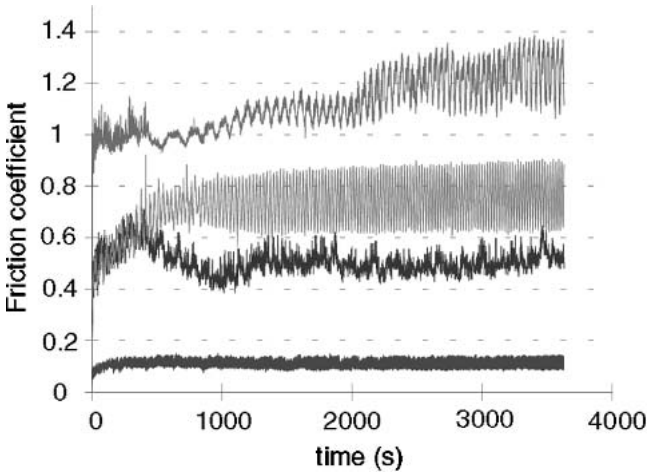

Fig. 7 Time evolution of the friction coefficient of two bulk materials and two coatings. Slip velocity, 0.1 m/s; load, 3.7 N; (1 substrate of AU4G; 2, bulk steel; 3, sprayed steel; 4, sprayed steel + graphite)

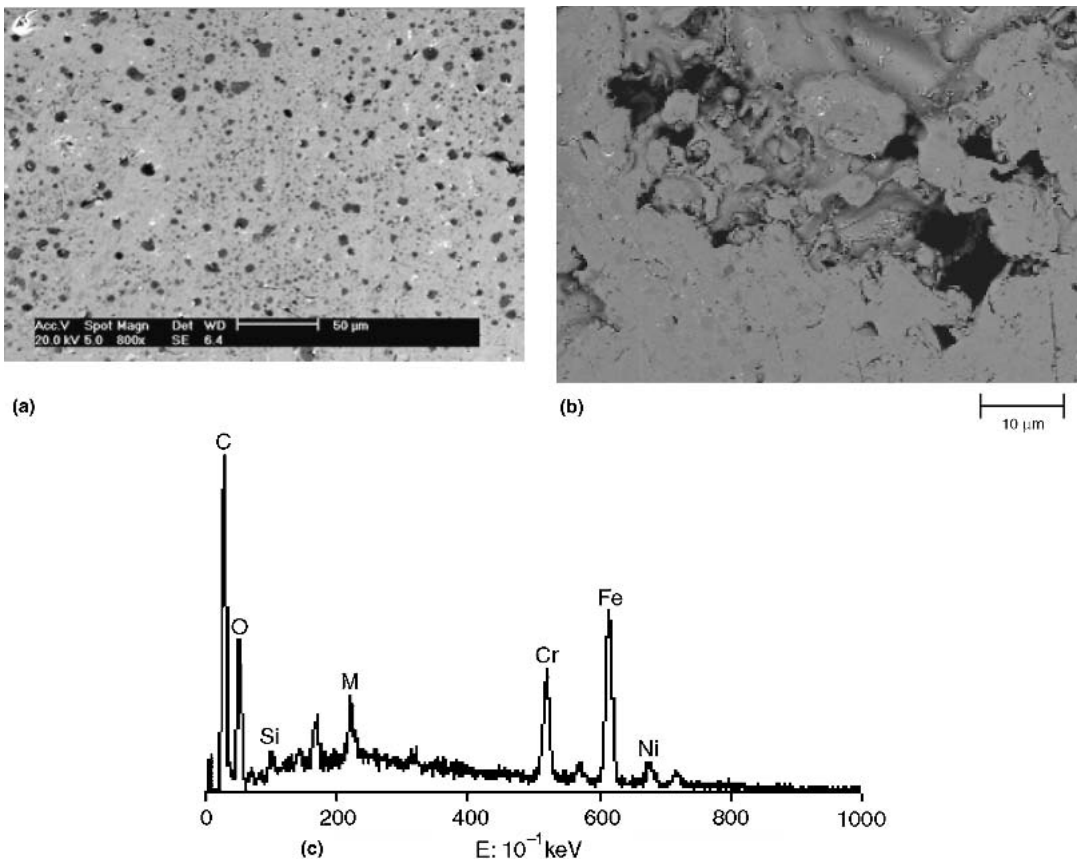

Fig. 8 SEM picture of the composite deposit of stainless steel-graphite: **(a)** view of the deposit, **(b)** an large view of a dark inclusion, **(c)** EDS of the graphite inclusions

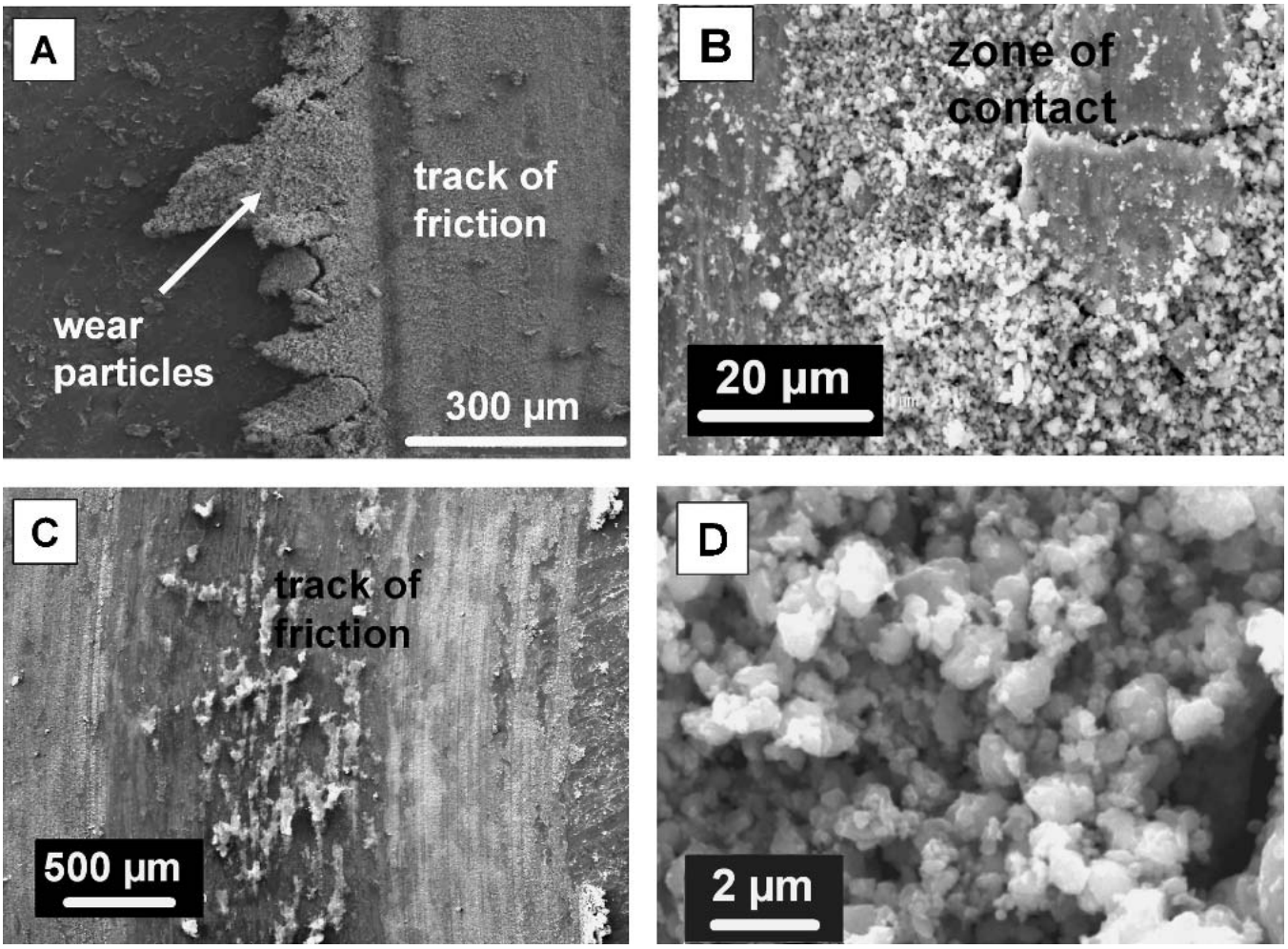

Fig. 9 Morphologies of the friction track at different scales for the composite coating. Slip velocity, 0.1 m/s; load, 3.7 N

3.5 Composite Coatings Through Graphite Injection Within a Specific Device

To achieve better control of the graphite injection, a special guide was designed to limit blow-out of the deposited graphite layer on the substrate. This guide, in contact with the rotating substrate, uniformly distributes the graphite as shown in Fig. 8(a). Figure 8(b) shows that porosity exists around the imbedded graphite particles. The local EDS analysis of these inclusions (Fig. 8c) shows, prominently, the K_α x-ray peak for graphite. However, the small diameter of these inclusions makes their analysis difficult, with peaks for iron, chromium, and nickel from the stainless steel also visible.

With this system it is possible to achieve a volume percent between 1 and 12. In Fig. 7, the results obtained with pure aluminium, bulk stainless steel, plasma sprayed stainless steel, and the composite coating are presented.

As expected, the aluminium substrate is ploughed severely by the 100C6 pin, and results are meaningless. The bulk stainless steel has a higher friction coefficient than that of the stainless steel sprayed material. This is probably due to the presence of oxide particles at the interface. The composite coating exhibits a significant improvement in f (~0.1 as compared with 0.45 for sprayed stainless steel). Examination of the friction tracks (Fig. 9) shows the presence of a powdered third body, which is uniformly distributed all over the track and acts in the same way as a grease. The SEM and EDS analyses of the third body show the presence of graphite mixed with the stainless steel particles and they are roughly spherical.

Figures 10(a) to 10(c) show the results obtained when the load increases. At 11.7 N, the time variation of the friction coefficient of the composite coating is very stable but is three times higher than with a load of 3.7 N. With higher loads the time variation for f is not stable and higher values are obtained with the 18 N load than with the 28 N load. This behavior is characteristic of the evolution of the friction coefficient with the load.

4. Conclusion

The process of cospraying (i.e., plasma molten stainless steel and solid graphite particles injected with a specially designed guide) allows composite coatings made of graphite particles randomly distributed in a metallic matrix of stainless steel to be deposited on aluminum substrates. Such deposits

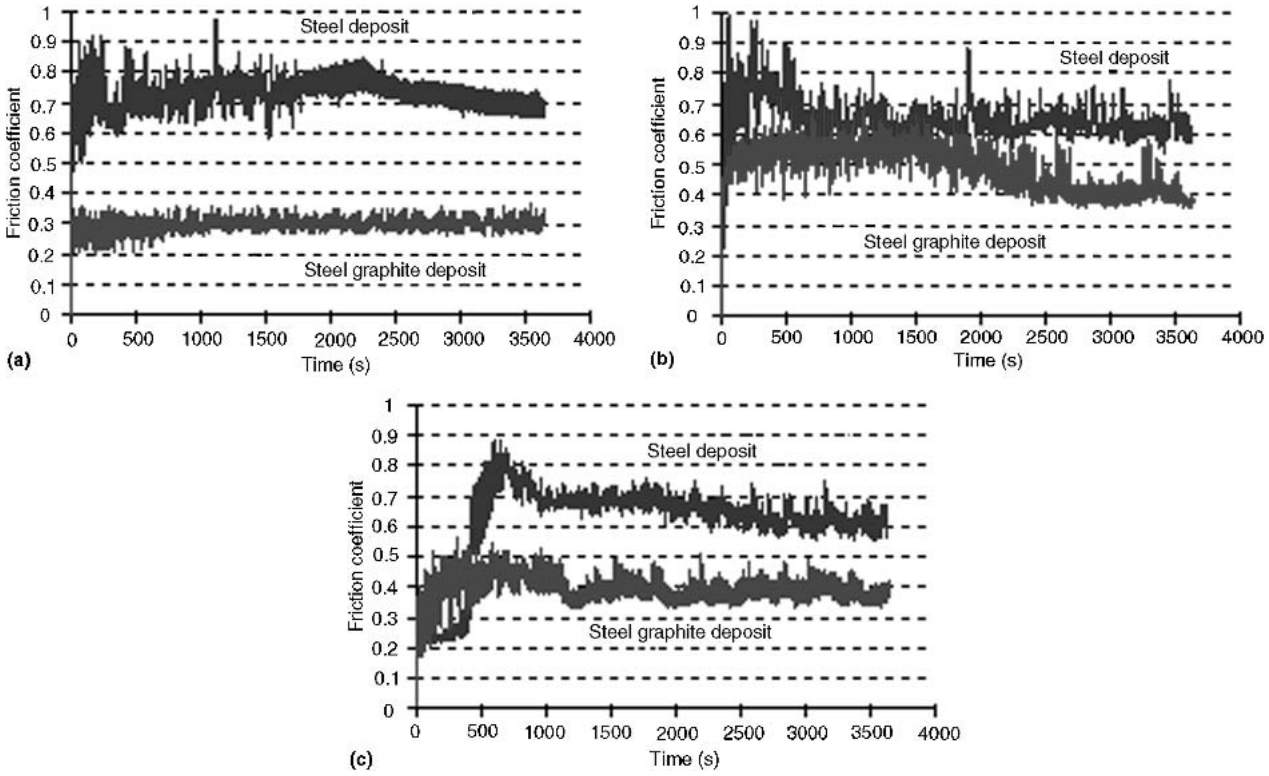

Fig. 10 Time evolution of the friction coefficient for a slip velocity of 0.1 m/s and 3 loads: **(a)** 11.7 N, **(b)** 18 N, **(c)** 28 N

show a lamellar structure and have a thickness on the order of 500 μm for a deposition time of 5 min with a stainless steel powder flow rate of 80 g/min.

Graphite particles are uniformly incorporated within the stainless steel coating for a volume fraction up to 12%. The coating hardness is about 3/4 that of the pure stainless steel with only 2 vol.% graphite. This seems to be the best compromise for a small (~6%) reduction of the coating hardness leading to a low friction coefficient. The dry friction coefficient, measured by using a 100C6 pin on a pin-on-disk test, is 1.5-4 times lower than that of the stainless steel coating. This is due to the presence of a third body that is uniformly distributed on the track surface. The third body particles are small (approximately a few microns in diameter), almost spherical, and made of stainless steel and graphite.

References

1. A. Borisova, Y. Borisov, A Tunik, L. Adeeva, E. Lugscheider, and C. Herbst, *Tagungsband Conference Proceedings,* E. Lugscheider and P.A. Kammer, Ed., ASM International, 1999, p 174-181
2. H.D. Steffens, J. Wilden, D. Hanmann, M. Granilick, M. Viwel, M. Höhle, and M.C. Nestler, *Thermal Spraying—Current States and Future Trends,* A. Ohmori, Ed., High Temp. Soc. Japan, Vol. 2, 1995, p 657-62
3. B.R. Marple and J. Voyer, *Thermal Spray: Surface Engineering via Applied Research,* C.C. Berndt, Ed., ASM International, 2000, p 909-918
4. S. Hartmann, F. Bültmann, and F. Janke, *Tagungsband Conference Proceedings,* E. Lugscheider and P.A. Kammer, Ed., ASM International, 1999, p 169-173
5. S.D. Siegmann, O.C. Brandt, and N.M. Margadant, *Thermal Spray: Surface Engineering via Applied Research,* C.C. Berndt, Ed., ASM International, 2000, p 1135-1140
6. J.M. Guilemany, J. Navarro, C. Lorenzana, S. Vizcaino, and J.M. Miguel, *Thermal Spray 2001: New Surfaces for a New Millennium,* C.C. Berndt, K.A. Khor, and E.F. Lugscheider, Ed., ASM International, 2001, p 1115-1118
7. A. Harir, "Contribution to the Feasibility of Plasma Spraying Steel-Solid Lubricant Composite Coatings and Their Tribological Behavior," Thèse de l'Université de Limoges, 2002 (in French)
8. M. Mellali, "Influence of the Surface Roughness and Substrate Temperature on the Adhesion and Residual Stress Distribution of Plasma Sprayed Alumina Coatings," Thèse de l'Université de Limoges, 1994 (in French)
9. H. Ageorges and P. Fauchais, *Thin Solid Films,* Vol 370, 2000, p 213-222
10. A.A. Syed, A. Denoirjean, P. Denoirjean, J.C. Labbe, P. Fauchais, In-Flight Oxidation of Stainless Steel Particles in Plasma Spraying, Invited paper accepted in Journal of Thermal Spray Technology, 2003
11. P. Reynaud and Y. Berthier: "Space Tribology, Friction Under Extreme Conditions," Senlis, F, November 21, 1992, CETIM Senlis, p 19
12. Y. Berthier, "Mechanisms and Tribiology," State Thesis, INSA Lyon, F, 1988 (in French)
13. M. Godet, Wear, *100,* 1984, p 437-52
14. P. Fournier, "Dry Friction of Monolithic Composite and Refractory Materials: Analysis Through the Concept of Body," l'Université de Limoges, 1997 (in French)